

1 **A novel superfamily of tube-like lipid transfer proteins**

2 Sarah D. Neuman¹, Tim P. Levine^{2*}, Arash Bashirullah^{1*}

3 1) Division of Pharmaceutical Sciences, University of Wisconsin-Madison, Madison, WI,
4 USA 53705-2222.

5 2) UCL Institute of Ophthalmology, University College London, 11-43 Bath Street,
6 London, EC1V 9EL, UK

7 *Correspondence: tim.levine@ucl.ac.uk (T.P. Levine) and bashirullah@wisc.edu (A.
8 Bashirullah)

9

10 Keywords: lipids, lipid transfer proteins, membrane contact sites, Vps13, autophagy,
11 AlphaFold

12

13 **Abstract**

14 Lipid transfer proteins mediate non-vesicular transport of lipids at membrane contact sites
15 to regulate the lipid composition of organelle membranes. Recently, a new type of rod-
16 like lipid transfer protein has emerged; these proteins contain a long hydrophobic groove
17 and can mediate bulk transport of lipids between organelles. Here we review recent
18 insights into the structure of these proteins and identify a repeating modular unit that we
19 propose to name the repeating β -groove (RBG) domain. This new structural
20 understanding conceptually unifies all the RBG domain-containing lipid transfer proteins
21 as members of a RBG protein superfamily. We also examine the biological functions of
22 these lipid transporters in normal physiology and disease and speculate on the
23 evolutionary origins of RBG proteins in bacteria.

24 **Non-vesicular lipid transfer occurs at membrane contact sites**

25 The lipid composition of each organelle membrane is unique and plays an
26 essential role in maintaining organelle identity and function. Lipids can be moved between
27 organelles via vesicular or non-vesicular trafficking. Seminal work in the 1980s suggested
28 that phospholipids and sterols are primarily transported via non-vesicular routes [1,2];
29 since then, evidence supporting the primacy and importance of non-vesicular lipid
30 transport has continued to grow. Non-vesicular lipid trafficking is carried out by lipid
31 transfer proteins (LTPs), cytoplasmic proteins that lower the energy barrier for lipids to
32 move between membranes across aqueous spaces [3].

33 Most known LTPs fold to form a box-like shape with a hydrophobic lining capable
34 of holding a single lipid [4,5]. These box-like LTPs transfer lipids via a shuttling
35 mechanism, selecting one lipid molecule at a time based on headgroup and transferring
36 it from donor to acceptor membranes [4]. Often this occurs at membrane contact sites,
37 locations where two organelles are in close enough proximity that a single protein can
38 bridge the gap [6].

39 In the last four years, a new class of LTP has emerged. These LTPs are large
40 proteins that fold to form long tube-like structures that span the entire distance between
41 membranes at membrane contact sites [7–13]. The hydrophobic lining of these tube-like
42 LTPs enables them to function like lipid superhighways connecting organelle membranes
43 [7,9,12,13]. Five members of this LTP family have been identified: VPS13, ATG2, the Hob
44 proteins, Tweek/Csf1/KIAA1109 and SHIP164 [7–9,12–18]. In this review, we examine
45 recent advances in understanding the structure of this novel superfamily of tube-like
46 LTPs, highlighting a shared structural feature composed of a repeating series of β -sheets

47 that we call the repeating β -groove (RBG) domain. We also review recent developments
48 in characterizing the molecular, cellular and physiological functions of these proteins and
49 speculate on their evolutionary origins.

50

51 **A new family of eukaryotic LTPs with long hydrophobic grooves**

52 VPS13 and ATG2 are large (3000-4000 and ~2000 amino acids, respectively)
53 proteins that are highly conserved among eukaryotes. Structural studies in the last four
54 years showed that both proteins fold to form a rod with an internal hydrophobic cavity
55 along its length. A crystal structure of the N-terminal 300 residues of fungal VPS13
56 revealed a β -sheet curved into a U-shape; crucially, the interior of the “U” was
57 hydrophobic, while the exterior was hydrophilic [7]. This work was followed by single
58 particle cryo-electron microscopy (EM) studies of a much longer fragment (N-terminal
59 1400 amino acids), which showed that the curved β -sheet structure continued down the
60 length of the protein to form a long hydrophobic groove [9] (Fig. 1). A crystal structure of
61 an N-terminal fragment of ATG2 [13] and cryo-EM analysis of full-length human ATG2A
62 [12] also found a similar long hydrophobic groove (Fig. 1). Importantly, VPS13 and ATG2
63 were shown to transfer lipids *in vitro* [7,11–13,19]. Thus, these two proteins were the
64 founding members of a new superfamily of LTPs with long hydrophobic grooves.

65 Three additional members of this novel LTP superfamily were recently uncovered.
66 SHIP164 (also called UHRF1BP1L; 1200-1500 residues) was identified via sequence
67 homology and cryo-EM as a VPS13-like protein conserved in all eukaryotes except fungi
68 [14]. Two additional long hydrophobic groove LTPs were identified via remote homology
69 to VPS13/ATG2 using HHpred [20]: Tweek and the Hob proteins [16,17]. Like the other

70 rod-like LTPs, both are large proteins (3000-5000 and 2300-3000 residues, respectively).
71 Tweek (Csf1 in *Saccharomyces cerevisiae*, KIAA1109 in humans) is conserved in fungi
72 and metazoans (opisthokonts); the Hob proteins (Hobbit in *Drosophila melanogaster*,
73 KIAA0100 in humans, SABRE/KIP and APT1 in plants) are conserved throughout
74 eukaryotes. The homology searches were confirmed upon release of the protein structure
75 prediction program AlphaFold [21], which predicts that Tweek and the Hob proteins fold
76 to form rods with internal hydrophobic grooves, structures with marked similarity to VPS13
77 and ATG2 (Fig. 1). Modeling by trRosetta, another high-performing protein folding
78 prediction program [22], produced similar structures [16]. While there are some caveats
79 that must be considered when working with protein prediction programs, they are highly
80 accurate for folded domains (Box 1). The most conspicuous feature of all five tube-like
81 LTPs is an extended run of U-shaped β -sheets that together forms the hydrophobic
82 groove (Fig. 1).

83

84 **The repeating β -groove (RBG) domain: a modular building block of long** 85 **hydrophobic groove LTPs**

86 Analysis of the predicted AlphaFold structures for VPS13, ATG2, Hobbit, Tweek
87 and SHIP164 reveals an intriguing pattern: all the hydrophobic grooves are composed of
88 a simple modular unit that oligomerizes head-to-tail to build a long rod. The module
89 contains five antiparallel β -strands followed by a sixth element consisting of a disordered
90 loop usually starting with a short helix that curves back across the β -sheet (Fig. 2A-D).
91 The β -strands form a U-shape by bending at a 30-60° angle at their mid-points, which are
92 frequently populated by strand-breaking residues (glycine/proline) (Fig. 2B-C).

93 Importantly, the residues populating the inner face of the U-shaped β -sheet are
94 hydrophobic, while those on the exterior face are hydrophilic (Fig. 2C). Multimerization of
95 these repeating units creates an unbroken chain of structurally identical repeats that
96 together build the hydrophobic groove (Fig. 2A, D). This pattern of repeating units had
97 already been seen in the high resolution cryo-EM structure of ATG2 [12], validating the
98 AlphaFold predictions. We propose to call this repeating module of five antiparallel β -
99 strands followed by a loop the repeating β -groove (RBG) domain and LTPs with long
100 hydrophobic grooves RBG proteins.

101 Each RBG protein is composed of a characteristic number of RBG domains (from
102 six in SHIP164 to 17 in Tweek; Fig. 2E). The number of RBG domains in each RBG
103 protein is highly conserved across orthologous proteins in different species. RBG
104 domains form superhelices in the RBG proteins, since each β -strand is rotated 6-8°
105 (anticlockwise looking from the N-terminus) compared to the previous. The modeled
106 superhelices point at different angles from the protein's long axis: Tweek and the Hob
107 proteins are the straightest, while ATG2 and VPS13 are predicted to have greater offset
108 angles (Fig. 3A). The significance of the modeled offset angles is unknown, but if verified,
109 they would alter the diameter of the superhelix (Fig. 3A) and, together with the number of
110 RBG domains, affect the overall length of the protein. This may affect which inter-
111 organellar gaps the RBG proteins can span.

112 The basic structure of the RBG domain (five β -strands plus a loop) is modified in
113 some modules, often in the length of the loop and uncommonly in the number of β -
114 strands. In all RBG proteins, the N-terminal RBG domain has a helix in place of the first
115 β -strand, while the C-terminal RBG domain is shortened, containing only two β -strands

116 in VPS13, ATG2 and the Hob proteins and one or three β -strands in Tweek and SHIP164,
117 respectively (Fig. 2E). In VPS13, ATG2, SHIP164 and the Hob proteins, all RBG domains
118 in the middle of the protein contain the characteristic five-stranded β -sheet structure. By
119 contrast, in Tweek, two of the central RBG domains contain only three β -strands and a
120 third RBG domain contains seven β -strands (Fig. 2E). The loop element of RBG domains
121 always occurs after an odd number of β -strands, maintaining the symmetry of the
122 structure so that the multimerization that extends the hydrophobic groove is uninterrupted.
123 The final loop element of the RBG domain is most often composed of a single helix and
124 a short, disordered polypeptide chain. But in some cases, the length of the final element
125 varies widely, even encoding an entire domain >700 amino acids long that extends away
126 from the hydrophobic groove. These additions to the hydrophobic groove are conserved
127 across orthologous RBG proteins, suggesting that they play a role in the function and/or
128 localization of RBG proteins [23].

129

130 **Molecular functions of the eukaryotic RBG proteins: Lipid superhighways**

131 The hydrophobic groove of RBG proteins, which seems *a priori* capable of lipid
132 transport, has had this function confirmed via *in vitro* analysis of glycerophospholipid
133 transport by VPS13, ATG2 and SHIP164 [7,11–14,19]. Although lipid transport has not
134 yet been assayed for Tweek or the Hob proteins, the marked structural similarity shared
135 among RBG proteins suggests that all are likely to perform the same function. Small box-
136 like LTPs contain a hydrophobic pocket capable of harboring only one lipid [4,5]; in
137 contrast, the hydrophobic cavity formed by the RBG fold is large enough to accommodate
138 tens of glycerophospholipids at a time [9,12]. In ATG2 and VPS13, mutation of a band of

139 hydrophobic residues within the groove to hydrophilic residues inhibits lipid transfer
140 activity [9,12]. Thus, it seems highly likely that a primary molecular function of RBG
141 proteins is bulk transport of lipids along hydrophobic grooves.

142 Despite many advances in our understanding of the molecular function of RBG
143 proteins in the last few years, there are still many unknowns about the selection, direction
144 and energetics of lipid transfer. VPS13 and ATG2 take part in reactions that transfer lipids
145 from the N- to the C-terminus [7,12,14], while Tweek/Csf1 has been suggested to
146 transport lipids, including phosphatidylethanolamine (PE), in the opposite direction from
147 the C- to the N-terminus [16]. The mechanisms that determine the directionality of lipid
148 transfer remain largely unknown. ATG2 was recently shown to physically interact with
149 lipid scramblases in both the donor and acceptor compartments for ER to autophagosome
150 lipid transport (TMEM41B/VMP1 and ATG9, respectively) [24]. Scramblases may play a
151 role in dissipating concentration gradients between the inner and outer leaflets of the
152 recipient membranes as lipids arrive. Human VPS13A also interacts with the lipid
153 scramblase XK [25]. Whether Tweek or the Hob proteins interact with scramblases is
154 unknown. Regarding lipid selectivity, it is possible that properties intrinsic to the RBG
155 proteins, in particular the highly conserved sequences at the N- or C-termini (Box 2), play
156 a role in selecting lipid moieties for subsequent transport through the channel; however,
157 this has not yet been tested. Future studies will no doubt examine the molecular
158 mechanisms that govern selectivity and directionality of lipid transport by RBG proteins.

159

160 **Cellular functions of the RBG proteins: Membrane biogenesis and lipid**
161 **homeostasis**

162 Membrane contact sites are often detected by the close apposition (10-30 nm) of
163 two different organelle membranes; these appositions are critical regions for integration
164 of cellular function and physiology and are the primary sites of action for many LTPs [6].
165 Accordingly, most of the RBG proteins have been detected at one or more membrane
166 contact sites *in vivo* (Table 1). To date, RBG proteins have been implicated in two types
167 of cellular processes: *de novo* generation of membranes and lipid homeostasis.

168 ATG2 and VPS13 function in *de novo* membrane synthesis. ATG2 is primarily
169 implicated in macroautophagy, an essential cellular process that drives non-selective
170 degradation of cellular detritus, including protein aggregates and defective organelles
171 [26]. Autophagy requires the formation of a new double-membraned organelle, the
172 autophagosome, which encapsulates cellular debris in an isolation membrane that fuses
173 with lysosomes for content degradation [12,26]. Recent studies show that ATG2 localizes
174 to endoplasmic reticulum (ER)-autophagosome membrane contact sites in yeast and
175 human cells, where it drives expansion of the isolation membrane [12,13]. Thus, the
176 specific subcellular localization of ATG2, coupled with its putative bulk lipid transfer
177 capabilities, likely confers the ability to generate new membrane and form
178 autophagosomes largely from scratch. Similarly, one of the functions of VPS13 is pro-
179 spore membrane expansion during *S. cerevisiae* meiosis [27]. VPS13 is enriched at the
180 pro-spore membrane during sporulation [27] and may form a bridge connecting this
181 membrane directly or indirectly to lipid droplets, which are hypothesized to serve as a
182 source of lipids for pro-spore membrane biogenesis [28]. A significant feature of both the
183 autophagic isolation membrane and the yeast pro-spore membrane is that they are lipid-
184 rich and protein-poor compared to most organelles. For example, autophagosomes have

185 just one integral membrane protein, ATG9, which is the membrane receptor for ATG2
186 [24]. The mechanism driving bulk lipid traffic to generate protein-poor membranes
187 remained elusive until the discovery of VPS13 and ATG2.

188 Other RBG proteins appear to function in lipid homeostasis. Defects in the
189 subcellular distribution of PI(4,5)P₂ (normally highly enriched on the plasma membrane)
190 are observed in *D. melanogaster hobbit* mutant cells, with Hobbit (and its yeast orthologs)
191 localizing to ER-plasma membrane contact sites in both organisms [18]. Mutation of
192 *hobbit* also results in cell-autonomous defects in regulated exocytosis by professional
193 secretory cells; these defects are caused by aberrations in trafficking of membrane fusion
194 proteins, which are absent from secretory granule membranes [29]. *tweek* mutant cells
195 also exhibit defects in the levels and subcellular distribution of PI(4,5)P₂ and in
196 endocytosis of synaptic vesicles [30]. A recent study demonstrated that *S. cerevisiae* Csf1
197 (and its human and *Caenorhabditis elegans* orthologs) plays a role in delivering PE to the
198 ER for synthesis of glycosylphosphatidylinositol (GPI) anchors [16], and other work also
199 suggests a role for yeast Csf1 in lipid homeostasis [31]. SHIP164 appears to function in
200 endocytic/retrograde trafficking of specific cargo proteins [14]. Understanding the
201 connection between lipid trafficking and cellular phenotypes will require further
202 investigation.

203 The function of RBG proteins is dictated by their localization to specific membrane
204 contact sites. This has stimulated research into mechanisms that regulate the subcellular
205 localization of RBG proteins. Sequence motifs that bind lipids and/or organelle-specific
206 adapter proteins have been identified at the N- and C-termini of the VPS13 and Hob
207 proteins [7,8,15,18,32–34]. However, this work is just beginning, and the full complement

208 of intrinsic and extrinsic factors driving RBG protein localization remains to be uncovered.
209 Additionally, the kinetics and stability of RBG protein localization to membrane contact
210 sites is unknown. Do RBG proteins constitutively localize to their target membrane contact
211 site, or are they dynamically recruited when their function is needed, and what is the
212 regulatory mechanism?

213

214 **Physiological and developmental functions of the RBG proteins: Mysterious** 215 **drivers of disease**

216 All experimental evidence to date points to lipid transport as the primary molecular
217 function of RBG proteins, but the significance of this process for organismal development
218 and physiology remains poorly understood. Mutations in several RBG proteins are
219 associated with human diseases; thus, by uncovering the developmental and
220 physiological roles of these proteins, we will gain valuable insights into the etiology of
221 these conditions.

222 There is a strong connection between mutation of RBG proteins and neurological
223 disease. Mutations in VPS13A are associated with the neurodegenerative disease
224 chorea-acanthocytosis [35], VPS13B with the neurodevelopmental disease Cohen
225 syndrome [36], VPS13C with early-onset Parkinson's disease [37] and VPS13D with
226 spastic ataxia [38]. Mutations in the human ortholog of *tweek* (*KIAA1109*) cause the
227 neurodevelopmental disorder Alkuraya-Kučinskas syndrome [39]. However, the
228 relationship between the putative lipid transfer function of these proteins and disease has
229 not yet been uncovered.

230 Although mutation of the human Hob protein (*KIAA0100*) has not yet been
231 associated with disease, the developmental and physiological roles of the Hob proteins
232 have been extensively characterized in *D. melanogaster* and in plants. In *D.*
233 *melanogaster*, *hobbit* is an essential gene, as loss-of-function *hobbit* mutant animals
234 exhibit a dramatic reduction in pupal body size (leading to the name) and lethality during
235 metamorphosis [29]. The small body size of *hobbit* mutant animals is caused by defects
236 in the endocrine signaling axis that drives release of insulin [29], which regulates both
237 carbohydrate metabolism and systemic growth in flies [40]. However, rescue of body size
238 via restoration of this endocrine signaling axis does not rescue the lethality of *hobbit*
239 mutant animals [29], showing that additional vital functions of *hobbit* are yet to be
240 uncovered. In a fascinating parallel, systemic stunted growth also results from mutation
241 of plant orthologs of *hobbit*, including loss of *SABRE* and *KIP* in *Arabidopsis thaliana* and
242 loss of *SABRE* in *Physcomitrium patens* [41–44]. *A. thaliana* *SABRE/KIP* mutants also
243 exhibit defects in root hair patterning [44] and abnormal elongation of pollen tubes [43], a
244 phenotype shared in mutants of the *Zea mays* Hob protein *APT1* [45]; *P. patens* *SABRE*
245 mutants also have defective cell plate deposition [42]. Root hair growth, pollen tube
246 elongation and cell plate deposition all rely heavily on the secretory pathway [46–48].
247 Given that fly *hobbit* function is required for regulated exocytosis in professional secretory
248 cells (as mentioned in the previous section) [29], this reveals a possible conserved
249 requirement for the Hob proteins in secretory trafficking pathways.

250 Phenotypic analysis of mutant animals has also revealed that *D. melanogaster*
251 *Vps13* and *Tweek* have essential functions in animal development and physiology. Flies
252 have three *Vps13* genes: *Vps13* (similar to human *VPS13A/C* [49]), *Vps13B* and *Vps13D*.

253 *Vps13* knockouts are viable but exhibit reduced fertility and defects in nurse cell clearance
254 during oogenesis [50]. *Vps13D* mutants are lethal during larval/pupal stages (indicating
255 that *Vps13D* is an essential gene) and have defects in mitochondrial morphology [51].
256 Mutation of *tweek* usually results in lethality during metamorphosis, but a few flies survive
257 to adulthood and exhibit severe locomotion deficits and seizures [30]. These phenotypes
258 provide a foothold for future studies to connect the molecular and cellular functions of
259 VPS13 and Tweek/KIAA1109 to their role in physiology and disease.

260 Although the developmental and physiological manifestations of RBG protein
261 mutation are varied, one common theme emerges: all these proteins appear to be
262 required during cellular processes that depend heavily on lipid homeostasis and
263 membrane dynamics. VPS13 and ATG2 appear to drive *de novo* membrane formation,
264 while the Hob proteins, Tweek and SHIP164 seem to regulate the subcellular distribution
265 of lipids, including phosphoinositides, which are essential for organelle identity.
266 Unsurprisingly, loss of the Hob proteins, Tweek or SHIP164 results in aberrations in
267 intracellular trafficking. Some major questions remain. Why are some RBG proteins
268 essential genes (required for survival to adulthood in humans or animal models) [29],
269 while others are not [50]? Perhaps surprisingly, deletion of all five yeast RBG proteins
270 had no effect on growth on rich medium [16], but the complex phenotypes associated with
271 loss of VPS13, ATG2, Hobbit or Tweek in animals suggest that there is little redundancy
272 between RBG proteins. There may also be additional functions for RBG proteins beyond
273 lipid transfer, perhaps in transport of other biomolecules [52]. Future studies that answer
274 these questions will address the developmental and physiological roles of RBG proteins.
275

276 **Evolutionary origins of RBG proteins: prototypes in prokaryotes**

277 Because four of the RBG proteins (VPS13, ATG2, Hobbit and SHIP164) are conserved
278 across eukaryotes, all of these were likely present in the last eukaryotic common ancestor
279 (LECA). Interestingly, structurally similar proteins are also present in the intermembrane
280 space of Gram-negative bacteria [53–56]. The *Escherichia coli* protein TamB has been
281 shown by crystallography to have a C-terminus forming a β -groove with a hydrophobic
282 interior. Sequence analysis suggests that this structure is shared by the remainder of the
283 protein [52], which forms an elongated rod [55]. This suggests that RBG proteins first
284 arose in prokaryotes. Accordingly, analysis of the AlphaFold predictions for TamB and
285 other related proteins in Gram-negative bacteria reveals groove-like structures
286 resembling RBG proteins, built from a series of modules formed from β -strands and a
287 loop (Fig. 3B). While the number of β -strands per repeat is more variable and generally
288 larger (median of 11) than the eukaryotic RBG domain, a key feature shared with the
289 eukaryotic RBG domain is that the number of β -strands between each loop that crosses
290 the hydrophobic groove is always odd. This results in the bacterial RBG proteins having
291 a similar, though less modular, structure to the eukaryotic RBG proteins.

292 Further evolutionary links between bacterial and eukaryotic RBG proteins are
293 found in proteins that form elongated hydrophobic grooves in mitochondria and
294 chloroplasts, organelles that arose by endosymbiosis. Mdm31 is a protein present in the
295 mitochondrial inner membrane space in many fungi and some protists. This protein
296 contains an N-terminal transmembrane helix (required for anchoring to the inner
297 mitochondrial membrane [57]) followed by two RBG domains and a second
298 transmembrane helix; the AlphaFold structure suggests this second helix may integrate

299 into the outer mitochondrial membrane (Fig. 3B). TIC236 is a highly conserved protein
300 present in the chloroplast intermembrane space [58]. The predicted AlphaFold structure
301 of TIC236 is strikingly similar to TamB. The RBG domains of Mdm31 and TIC236 display
302 intermediate characteristics between prokaryotic and eukaryotic RBG domains. Like the
303 bacterial proteins, Mdm31 and TIC236 have variable numbers of β -strands per RBG
304 domain, but like the eukaryotic proteins, loops in the RBG domains tend to be longer,
305 adding structural complexity. Together, this structural evidence strongly suggests that
306 RBG proteins first arose in prokaryotes and evolved into the eukaryotic proteins we see
307 today.

308

309 **Concluding remarks**

310 The RBG proteins are a fascinating new family of bulk lipid transporters. Continued work
311 examining the molecular and cellular functions of these proteins is certain to reveal novel
312 roles for lipid trafficking at membrane contact sites, and many questions remain
313 unanswered (see Outstanding Questions). In the future, it will be particularly important to
314 characterize the developmental and physiological roles of RBG proteins since these
315 studies likely hold the key to understanding how mutation of these proteins causes human
316 disease.

317

318 **Acknowledgements**

319 We thank Amy Cavanagh for assistance with illustrations and Rosario Valentini, Maya
320 Schuldiner, Jerry Yang and Will Prinz for sharing original PDB files.

321 **Box 1. Considerations for interpretation of AlphaFold structures.**

322 AlphaFold2, as the first computational tool capable of predicting protein structures with
323 near-experimental accuracy [21], has undoubtedly contributed a striking advance in our
324 understanding of protein folding in general and particularly in understanding the structure
325 of long hydrophobic groove LTPs. However, it is not perfect [59]. When interpreting
326 AlphaFold predictions like those for the proteins under review here, significant issues
327 remain. One is that large proteins are generally not pre-made in the AlphaFold database.
328 In the *S. cerevisiae* proteome, the ten largest proteins (>2700 amino acids long, including
329 Vps13 and Csf1) are all absent. This problem can be circumvented by submitting
330 overlapping segments (up to 1000 amino acids) to the ColabFold version of AlphaFold2
331 [60] or to trRosetta [22]. The overlapping regions of the partial models can then be
332 assembled to generate a full-length prediction. This approach was used to generate the
333 models of Vps13 and Tweek shown in this review and in other recent publications [16,17].
334 A second issue is that AlphaFold provides visualizations of 100% of each protein, even
335 those regions that are predicted with a very low degree of confidence. This particularly
336 applies to unstructured loops. Even short loops are typically missing from experimentally
337 determined structures since they are too mobile to be visualized by crystallography,
338 nuclear magnetic resonance (NMR) imaging or single particle cryo-EM. While having
339 everything predicted is useful for creating complete structures of proteins with multiple
340 short loops like those seen in this family of LTPs, longer loops likely exist in a wide range
341 of positions *in vivo*. Thus, specification of a single conformation by AlphaFold must be
342 interpreted with caution. A related issue arises in protein regions where there is no strong
343 prediction for secondary structure or any intra-chain interactions. In these situations,

344 AlphaFold tends to predict unstructured loops by default. However, these loops usually
345 do not conform to the stereochemical rules that apply to polypeptide chains, meaning that
346 these they might best be viewed as arbitrary linkers [59]. Although it is critical to keep
347 these caveats in mind when analyzing structural predictions, AlphaFold is a remarkable
348 and powerful tool for folded domains.

349

350 **Box 2. Examining domains within RBG proteins.**

351 Domains have traditionally been defined based on conservation of sequence, and most
352 existing domain databases use sequence conservation as their main criterion for domain
353 detection. Domains have also typically been thought of as independent structural
354 modules. However, the low-throughput nature of traditional structural biology techniques
355 has made it impractical to solve the structure of every annotated domain; thus, until the
356 release of a reliable prediction program like AlphaFold, it had not been possible to fully
357 understand the relative importance of conserved sequences versus conserved structures
358 in defining protein domains. The RBG proteins provide an example of this issue. Domain
359 databases annotate an Apt1 domain near the C-terminus of Hobbit; this domain was
360 named for its presence in the C-terminal region of the *Z. mays* Hob protein APT1 [45].
361 The remote homology detection program HHpred [20] also detects an Apt1 domain near
362 the C-terminus of VPS13 and ATG2 [32,34,61]. The AlphaFold predictions show that the
363 Apt1 domain folds as an integral part of the hydrophobic groove (the final three RBG
364 domains make up the Apt1 domain; see Fig. 2A). Therefore, it is not an independent
365 structural domain. Yet, this C-terminal region is highly conserved both in terms of
366 sequence and in the potentially significant activity of binding the headgroups of

367 phosphoinositide lipids *in vitro* (with varying specificity) [18,32,34,61]. Thus, the Apt1
368 domain may be an independent functional unit, even though there is no recognizable
369 distinction in the predicted folding of the Apt1 domain compared to the rest of the RBG
370 protein. So far, no other regions of the RBG proteins besides the Apt1 domain bind
371 phosphoinositides [7,12,18], suggesting that lipid binding is dictated by conserved protein
372 sequences, not by protein structure. Future work will be required to confirm this
373 hypothesis. Standard domain databases also annotate other domains within the RBG
374 proteins, such as the Chorein_N domain in VPS13, ATG2 and SHIP164 (the first RBG
375 repeat makes up the Chorein_N domain; see Fig. 3A). Like the Apt1 domain, Chorein_N
376 domains fold contiguously with the hydrophobic groove, making it difficult to classify them
377 as distinct structural domains. Chorein_N domains may have a distinct function, though,
378 since specific conserved sequences within this domain are required for ATG2 localization
379 to the ER [62]. Thus, conserved sequences in the context of overall protein structure may
380 be the most critical feature in defining the function of some RBG protein domains.

381 Table 1. Reported subcellular localization of RBG proteins.

A) Eukaryotic RBG Proteins

RBG family	Gene name	Species	Localization	Ref.
Vps13	Vps13	<i>S. cerevisiae</i>	vacuole to mitochondria (vCLAMP)	[63,64]
			nuclear ER to vacuole (NVJ)	[23,63]
			endosome to mitochondria	[64]
			pro-spore membrane	[27,64]
			vacuole	[23,63,64]
			endosome	[23,63]
			peroxisome	[65]
			mitochondria	[63–65]
	VPS13A	<i>T. thermophila</i>	phagosome	[66]
	Vps13 (~Hs A/C)	<i>D. melanogaster</i>	ER to PM*	[50]
	Vps13D	<i>D. melanogaster</i>	lysosome	[51]
	VPS13A	<i>H. sapiens</i>	ER to mitochondria	[7,67,68]
			ER to lipid droplet	[7,67]
	VPS13B	<i>H. sapiens</i>	mitochondria to endosome	[68]
			Golgi	[69]
	VPS13C	<i>H. sapiens</i>	endosomes	[70]
ER to lipid droplet			[7]	
VPS13D	<i>H. sapiens</i>	ER to endo-lysosome	[7]	
		ER to mitochondria	[8]	
		peroxisomes	[8]	
Atg2	Atg2	<i>S. cerevisiae</i>	Golgi	[8,71]
			pre-autophagosomal structure (PAS)	[72]
	ATG2A	<i>H. sapiens</i>	ER to autophagosome	[12,73]
			lipid droplet	[73,75]
Hobbit	Fmp27 (Hob1)	<i>S. cerevisiae</i>	ER to mitochondria	[16,18]
			PM-lipid droplet (pCLIP) [#]	[16]
			ER-lipid droplet (LiDER) [#]	[17]
			ER-lipid droplet (LiDER) [#]	[17]
	Hob2 (Ypr117w)	<i>S. cerevisiae</i>	ER to PM	[16,18]
			ER to mitochondria	[16]
			PM-lipid droplet (pCLIP) [#]	[17]
	Hobbit	<i>D. melanogaster</i>	ER-lipid droplet (LiDER) [#]	[17]
SABRE	<i>P. patens</i>	ER to PM	[18]	
		ER (puncta)	[42]	

	SABRE	<i>A. thaliana</i>	PM	[41]
Tweek	Csf1	<i>S. cerevisiae</i>	ER to PM	[16]
			ER to mitochondria	[16]
			PM-lipid droplet (pCLIP) [#]	[17]
			ER-lipid droplet (LiDER) [#]	[17]
SHIP164	SHIP164	<i>H. sapiens</i>	early endosomes	[14,76]
	UHRF1BP1		late endosomes	[14]

B) Prokaryotic RBG Proteins

TamB/ AsmA family	TamB	<i>E. coli</i>	inner to outer membrane	[54,77]
	AsmA			[77]
	YicH		inner membrane (to outer?)	[77]
	YhjG			[77]
	YdbH			[77]
	YhdP		outer membrane (to inner?)	[77]
TamB relatives in endo- symbionts	Mdm31	<i>S. cerevisiae</i>	inner mitochondrial membrane	[57]
	TIC236 (At2g25660)	<i>A. thaliana</i>	inner to outer chloroplast membrane	[58]

382

383 *ER to PM localization is inferred from a close association between Vps13 and both the
384 ER and PM. Direct co-localization with an ER-PM marker was not assessed.

385 [#]This localization was observed with N-terminally tagged RBG protein, which may disrupt
386 ER membrane insertion.

387 **Figure Legends**

388 **Figure 1. Long hydrophobic groove lipid transfer proteins share structural**
389 **similarities.** Ribbon models (top) and cross-sections of sphere models (bottom) showing
390 representative members of five protein families that consist of long tube-like structures
391 comprised primarily of β -sheets (labeled blue in ribbon models), which form a groove lined
392 with hydrophobic residues (glycine, alanine, valine, leucine, isoleucine, proline,
393 phenylalanine, methionine and tryptophan; labeled orange in sphere models). The origins
394 of the models are *S. cerevisiae* Vps13, *H. sapiens* ATG2A, *H. sapiens* Hobbit (KIAA0100),
395 *S. cerevisiae* Tweek (Csf1) and *H. sapiens* SHIP164. The SHIP164 rendering omits two
396 long unstructured loops (residues 873-1170 and 1360-1464). PDB files for Vps13 and
397 Csf1 were obtained from Jerry Yang and William Prinz, who used trRosetta to predict
398 regions of ~1000 amino acids, then assembled a complete model from overlapping
399 segments [16]. PDB files for ATG2A, Hob and SHIP164 were obtained from the AlphaFold
400 database [21]. All renderings were generated in ChimeraX [78]. Note that the VPS13
401 model contains a disconnect in the hydrophobic groove coincident with a large insertion
402 called the VAB domain ([23]; further discussed in Fig. 3).

403

404 **Figure 2. The “repeating β -groove” (RBG) domain is the modular building block of**
405 **RBG lipid transfer proteins. (A)** Ribbon model of *D. melanogaster* Hobbit with RBG
406 domains alternately labeled in pink, yellow and blue. Rendering generated using PyMOL
407 version 2.3.4. PDB file obtained from the AlphaFold database [21]. **(B)** Model of a single
408 RBG domain from *D. melanogaster* Hobbit showing the basic RBG domain structure
409 consisting of five antiparallel β -strands (blue) that form a groove, followed by an

410 unstructured loop that crosses back over the β -sheet (gray). Ribbon models: left – front
411 view, middle – side-view (90° rotation). Note the presence of strand-breaking residues
412 (colored pink) near the middle of each strand that generate curvature. **(C)** Sphere model
413 side-view of the same RBG domain in (B), demonstrating that the concave surface
414 (interior) of the RBG domain's groove is lined with hydrophobic residues (orange), while
415 the convex surface (exterior) is hydrophilic (gray). Strand-breaking residues shown in
416 pink. Models generated with ChimeraX [78]. **(D)** Cartoon illustration of three contiguous
417 RBG domains. The direction of each β -strand and loop is indicated by arrowheads. **(E)**
418 Illustration of the number of RBG domains present in each RBG protein family, as well as
419 the total length of each predicted protein. Note that the initial and final RBG domains are
420 shorter in each protein (indicated by “-”); additionally, Tweek contains two RBG domains
421 with three β -strands and one with seven β -strands (indicated by “+”).

422

423 **Figure 3. Structural features of RBG proteins in eukaryotes and prokaryotes. (A)**
424 Ribbon models of the five eukaryotic RBG proteins showing only β -sheets with long loops
425 and all helices omitted. Left: side-view shows that β -sheets of RBG proteins form
426 superhelices pointing at different angles relative to the long axis. This affects both overall
427 protein length and diameter, visible in an axial view (90° rotation, right). **(B)** Ribbon
428 models of YicH (*E. coli*) and Mdm31 (mitochondrial protein) highlight structural similarities
429 with eukaryotic RBG proteins. RBG domains colored as Figure 2A, with terminal helices
430 in purple and predicted transmembrane helices in black. Note that Mdm31 is adapted to
431 integrating into both the inner and outer mitochondrial membranes. Renderings generated
432 using CCP4MG software (QtMG package). PDB files for ATG2A (*H. sapiens*), Hobbit (*D.*

433 *melanogaster*), SHIP164 (*H. sapiens*), YicH (*E. coli*) and Mdm31 (*S. cerevisiae*, omitting
434 unstructured loops in residues 1-103, 188-224, 242-249, 358-368, 412-458) obtained
435 from AlphaFold database [21]. Tweek model is from *S. cerevisiae*, kindly provided by
436 Rosario Valentini [17]. VPS13 model was generated by submitting residues 1643-2111
437 and 2543-2840 from *S. cerevisiae* Vps13 (omitting 67% of the insert) to AlphaFold [60].
438 The resulting structure was overlapped with the AlphaFold model of *R. norvegicus*
439 VPS13A (residues 1-2335). Other published models of Vps13 ([16]; Fig. 1) show a
440 disconnect in the hydrophobic groove where the six VAB repeats (>700 residues; [23])
441 are inserted. Continuity traversing the VAB repeats as shown here is strongly predicted
442 (probability local distance difference test (pLDDT) values >0.9 [21]).

443 **References**

- 444 1 Kaplan, M.R. and Simoni, R.D. (1985) Intracellular transport of phosphatidylcholine
445 to the plasma membrane. *J. Cell Biol.* 101, 441–445
- 446 2 DeGrella, R.F. and Simoni, R.D. (1982) Intracellular transport of cholesterol to the
447 plasma membrane. *J. Biol. Chem.* 257, 14256–14262
- 448 3 Wirtz, K.W. and Zilversmit, D.B. (1968) Exchange of phospholipids between liver
449 mitochondria and microsomes in vitro. *J. Biol. Chem.* 243, 3596–3602
- 450 4 Wong, L.H. *et al.* (2019) Lipid transfer proteins: the lipid commute via shuttles,
451 bridges and tubes. *Nat. Rev. Mol. Cell Biol.* 20, 85–101
- 452 5 Wong, L.H. *et al.* (2017) Advances on the Transfer of Lipids by Lipid Transfer
453 Proteins. *Trends Biochem. Sci.* 42, 516–530
- 454 6 Prinz, W.A. *et al.* (2020) The functional universe of membrane contact sites. *Nat.*
455 *Rev. Mol. Cell Biol.* 21, 7–24
- 456 7 Kumar, N. *et al.* (2018) VPS13A and VPS13C are lipid transport proteins
457 differentially localized at ER contact sites. *J. Cell Biol.* 217, 3625–3639
- 458 8 Guillén-Samander, A. *et al.* (2021) VPS13D bridges the ER to mitochondria and
459 peroxisomes via Miro. *J. Cell Biol.* 220, e202010004
- 460 9 Li, P.Q. *et al.* (2020) Cryo-EM reconstruction of a VPS13 fragment reveals a long
461 groove to channel lipids between membranes. *J. Cell Biol.* 219, e202001161
- 462 10 Otomo, T. *et al.* (2018) The Rod-Shaped ATG2A-WIPI4 Complex Tethers
463 Membranes In Vitro. *Contact (Thousand Oaks)* 2018 Jan-Dec,
464 10.1177/2515256418819936
- 465 11 Maeda, S. *et al.* (2019) The autophagic membrane tether ATG2A transfers lipids

466 between membranes. *Elife* 8, e45777

467 12 Valverde, D.P. *et al.* (2019) ATG2 transports lipids to promote autophagosome
468 biogenesis. *J. Cell Biol.* 218, 1787–1798

469 13 Osawa, T. *et al.* (2019) Atg2 mediates direct lipid transfer between membranes for
470 autophagosome formation. *Nat. Struct. Mol. Biol.* 26, 281–288

471 14 Hanna, M.G. *et al.* (2021) SHIP164 is a Chorein Motif Containing Lipid Transport
472 Protein that Controls Membrane Dynamics and Traffic at the Endosome-Golgi
473 Interface . *bioRxiv* DOI: 10.1101/2021.11.04.467353

474 15 Neuman, S.D. *et al.* (2021) The Hob Proteins: Putative, Novel Lipid Transfer
475 Proteins at ER-PM Contact Sites. *Contact (Thousand Oaks)* 4, 1–3

476 16 Toulmay, A. *et al.* (2022) Vps13-like proteins provide phosphatidylethanolamine for
477 GPI anchor synthesis in the ER. *J. Cell Biol.* 221, e202111095

478 17 Castro, I.G. *et al.* (2021) Systematic analysis of membrane contact sites in
479 *Saccharomyces cerevisiae* uncovers modulators of cellular lipid distribution.
480 *bioRxiv* DOI: 10.1101/2021.10.17.464712

481 18 Neuman, S.D. *et al.* (2022) The Hob proteins are novel and conserved lipid-binding
482 proteins at ER-PM contact sites. *J. Cell Sci.* 135, jcs259086

483 19 Osawa, T. *et al.* (2020) Human ATG2B possesses a lipid transfer activity which is
484 accelerated by negatively charged lipids and WIPI4. *Genes to Cells* 25, 65–70

485 20 Gabler, F. *et al.* (2020) Protein Sequence Analysis Using the MPI Bioinformatics
486 Toolkit. *Curr. Protoc. Bioinforma.* 72, e108

487 21 Jumper, J. *et al.* (2021) Highly accurate protein structure prediction with AlphaFold.
488 *Nature* 596, 583–589

- 489 22 Yang, J. *et al.* (2020) Improved protein structure prediction using predicted
490 interresidue orientations. *Proc. Natl. Acad. Sci. U. S. A.* 117, 1496–1503
- 491 23 Bean, B.D.M. *et al.* (2018) Competitive organelle-specific adaptors recruit Vps13 to
492 membrane contact sites. *J. Cell Biol.* 217, 3593–3607
- 493 24 Ghanbarpour, A. *et al.* (2021) A model for a partnership of lipid transfer proteins
494 and scramblases in membrane expansion and organelle biogenesis. *Proc. Natl.*
495 *Acad. Sci. U. S. A.* 118, 2101562118
- 496 25 Park, J.S. and Neiman, A.M. (2020) XK is a partner for VPS13A: a molecular link
497 between Chorea-Acanthocytosis and McLeod Syndrome. *Mol. Biol. Cell* 31, 2425–
498 2436
- 499 26 Yu, L. *et al.* (2018) Autophagy pathway: Cellular and molecular mechanisms.
500 *Autophagy* 14, 207–215
- 501 27 Park, J.S. and Neiman, A.M. (2012) VPS13 regulates membrane morphogenesis
502 during sporulation in *Saccharomyces cerevisiae*. *J. Cell Sci.* 125, 3004–3011
- 503 28 Hsu, T.H. *et al.* (2017) Lipid droplets are central organelles for meiosis II
504 progression during yeast sporulation. *Mol. Biol. Cell* 28, 440–451
- 505 29 Neuman, S.D. and Bashirullah, A. (2018) Hobbit regulates intracellular trafficking
506 to drive insulin-dependent growth during *Drosophila* development. *Development*
507 145, dev161356
- 508 30 Verstreken, P. *et al.* (2009) Tweek, an Evolutionarily Conserved Protein, Is
509 Required for Synaptic Vesicle Recycling. *Neuron* 63, 203–215
- 510 31 John Peter, A.T. *et al.* (2021) Rewiring phospholipid biosynthesis reveals
511 robustness in membrane homeostasis and uncovers lipid regulatory players.

512 *bioRxiv* DOI: 10.1101/2021.07.20.453065

513 32 Rzepnikowska, W. *et al.* (2017) Amino acid substitution equivalent to human
514 chorea-acanthocytosis I2771R in yeast Vps13 protein affects its binding to
515 phosphatidylinositol 3-phosphate. *Hum. Mol. Genet.* 26, 1497–1510

516 33 Dziurdzik, S.K. and Conibear, E. (2021) The vps13 family of lipid transporters and
517 its role at membrane contact sites. *Int. J. Mol. Sci.* 22, 1–17

518 34 Kolakowski, D. *et al.* (2020) The binding of the APT1 domains to phosphoinositides
519 is regulated by metal ions in vitro. *Biochim. Biophys. Acta - Biomembr.* 1862,
520 183349

521 35 Ueno, S.I. *et al.* (2001) The gene encoding a newly discovered protein, chorein, is
522 mutated in chorea-acanthocytosis. *Nat. Genet.* 28, 121–122

523 36 Kolehmainen, J. *et al.* (2003) Cohen syndrome is caused by mutations in a novel
524 gene, COH1, encoding a transmembrane protein with a presumed role in vesicle-
525 mediated sorting and intracellular protein transport. *Am. J. Hum. Genet.* 72, 1359–
526 1369

527 37 Schormair, B. *et al.* (2018) Diagnostic exome sequencing in early-onset Parkinson's
528 disease confirms VPS13C as a rare cause of autosomal-recessive Parkinson's
529 disease. *Clin. Genet.* 93, 603–612

530 38 Koh, K. *et al.* (2020) VPS13D-related disorders presenting as a pure and
531 complicated form of hereditary spastic paraplegia. *Mol. Genet. Genomic Med.* 8,
532 e1108

533 39 Kumar, K. *et al.* (2020) KIAA1109 gene mutation in surviving patients with Alkuraya-
534 Kučinskis syndrome: A review of literature. *BMC Med. Genet.* 21, 1–11

535 40 Texada, M.J. *et al.* (2020) Regulation of body size and growth control. *Genetics*
536 216, 269–313

537 41 Pietra, S. *et al.* (2013) Arabidopsis SABRE and CLASP interact to stabilize cell
538 division plane orientation and planar polarity. *Nat. Commun.* 4, 1–15

539 42 Cheng, X. and Bezanilla, M. (2021) SABRE populates ER domains essential for
540 cell plate maturation and cell expansion influencing cell and tissue patterning. *Elife*
541 10, e65166

542 43 Procissi, A. *et al.* (2003) Kinky Pollen encodes a Sabre-like protein required for tip
543 growth in Arabidopsis and conserved among eukaryotes. *Plant J.* 36, 894–904

544 44 Pietra, S. *et al.* (2015) SABRE is required for stabilization of root hair patterning in
545 Arabidopsis thaliana. *Physiol. Plant.* 153, 440–453

546 45 Xu, Z. and Dooner, H.K. (2006) The maize aberrant pollen transmission 1 gene is
547 a SABRE/KIP homolog required for pollen tube growth. *Genetics* 172, 1251–1261

548 46 Guan, Y. *et al.* (2013) Signaling in pollen tube growth: crosstalk, feedback, and
549 missing links. *Mol. Plant* 6, 1053–1064

550 47 Smertenko, A. *et al.* (2017) Plant Cytokinesis: Terminology for Structures and
551 Processes. *Trends Cell Biol.* 27, 885–894

552 48 Hochholdinger, F. *et al.* (2018) Genetic Control of Root System Development in
553 Maize. *Trends Plant Sci.* 23, 79–88

554 49 Ugur, B. *et al.* (2020) Role of VPS13, a protein with similarity to ATG2, in physiology
555 and disease. *Curr. Opin. Genet. Dev.* 65, 61–68

556 50 Faber, A.I.E. *et al.* (2021) Vps13 is required for timely removal of nurse cell corpses.
557 *Dev.* 147, dev191759

558 51 Anding, A.L. *et al.* (2018) Vps13D Encodes a Ubiquitin-Binding Protein that Is
559 Required for the Regulation of Mitochondrial Size and Clearance. *Curr. Biol.* 28,
560 287-295.e6

561 52 Josts, I. *et al.* (2017) The Structure of a Conserved Domain of TamB Reveals a
562 Hydrophobic β Taco Fold. *Structure* 25, 1898-1906.e5

563 53 Levine, T.P. (2019) Remote homology searches identify bacterial homologues of
564 eukaryotic lipid transfer proteins, including Chorein-N domains in TamB and AsmA
565 and Mdm31p. *BMC Mol. Cell Biol.* 20, 43

566 54 Selkrig, J. *et al.* (2012) Discovery of an archetypal protein transport system in
567 bacterial outer membranes. *Nat. Struct. Mol. Biol.* 19, 506–510

568 55 Shen, H.H. *et al.* (2014) Reconstitution of a nanomachine driving the assembly of
569 proteins into bacterial outer membranes. *Nat. Commun.* 5, 1–10

570 56 Heinz, E. *et al.* (2015) Evolution of the translocation and assembly module (TAM).
571 *Genome Biol. Evol.* 7, 1628–1643

572 57 Dimmer, K.S. *et al.* (2005) Mdm31 and Mdm32 are inner membrane proteins
573 required for maintenance of mitochondrial shape and stability of mitochondrial DNA
574 nucleoids in yeast. *J. Cell Biol.* 168, 103–115

575 58 Chen, Y.L. *et al.* (2018) TIC236 links the outer and inner membrane translocons of
576 the chloroplast. *Nature* 564, 125–129

577 59 Jones, D.T. and Thornton, J.M. (2022) The impact of AlphaFold2 one year on. *Nat.*
578 *Methods* 19, 15–20

579 60 Mirdita, M. *et al.* (2021) ColabFold - Making protein folding accessible to all. *bioRxiv*
580 DOI: 10.1101/2021.08.15.456425

- 581 61 Kaminska, J. *et al.* (2016) Phosphatidylinositol-3-phosphate regulates response of
582 cells to proteotoxic stress. *Int. J. Biochem. Cell Biol.* 79, 494–504
- 583 62 Kotani, T. *et al.* (2018) The Atg2-Atg18 complex tethers pre-autophagosomal
584 membranes to the endoplasmic reticulum for autophagosome formation. *Proc. Natl.*
585 *Acad. Sci. U. S. A.* 115, 10363–10368
- 586 63 Lang, A.B. *et al.* (2015) ER-mitochondrial junctions can be bypassed by dominant
587 mutations in the endosomal protein Vps13. *J. Cell Biol.* 210, 883–890
- 588 64 Park, J.S. *et al.* (2016) Yeast Vps13 promotes mitochondrial function and is
589 localized at membrane contact sites. *Mol. Biol. Cell* 27, 2435–49
- 590 65 John Peter, A.T. *et al.* (2017) Vps13-Mcp1 interact at vacuole-mitochondria
591 interfaces and bypass ER-mitochondria contact sites. *J. Cell Biol.* 216, 3219–3229
- 592 66 Samaranyake, H.S. *et al.* (2011) Vacuolar protein sorting protein 13A, TtVPS13A,
593 localizes to the *Tetrahymena thermophila* phagosome membrane and is required
594 for efficient phagocytosis. *Eukaryot. Cell* 10, 1207–1218
- 595 67 Yeshaw, W.M. *et al.* (2019) Human VPS13A is associated with multiple organelles
596 and influences mitochondrial morphology and lipid droplet motility. *Elife* 8, e43561
- 597 68 Munõz-Braceras, S. *et al.* (2019) VPS13A is closely associated with mitochondria
598 and is required for efficient lysosomal degradation. *Dis. Model. Mech.* 12,
599 dmm036681
- 600 69 Seifert, W. *et al.* (2011) Cohen syndrome-associated protein, COH1, is a novel,
601 giant Golgi matrix protein required for Golgi integrity. *J. Biol. Chem.* 286, 37665–
602 37675
- 603 70 Koike, S. and Jahn, R. (2019) SNAREs define targeting specificity of trafficking

604 vesicles by combinatorial interaction with tethering factors. *Nat. Commun.* 10, 1–16

605 71 Baldwin, H.A. *et al.* (2021) Vps13d promotes peroxisome biogenesis. *J. Cell Biol.*
606 220, e202001188

607 72 Shintani, T. *et al.* (2001) Apg2p functions in autophagosome formation on the
608 perivacuolar structure. *J. Biol. Chem.* 276, 30452–30460

609 73 Velikkakath, A.K.G. *et al.* (2012) Mammalian Atg2 proteins are essential for
610 autophagosome formation and important for regulation of size and distribution of
611 lipid droplets. *Mol. Biol. Cell* 23, 896–909

612 74 Tang, Z. *et al.* (2019) TOM40 Targets Atg2 to Mitochondria-Associated ER
613 Membranes for Phagophore Expansion. *Cell Rep.* 28, 1744-1757.e5

614 75 Tamura, N. *et al.* (2017) Differential requirement for ATG2A domains for localization
615 to autophagic membranes and lipid droplets. *FEBS Lett.* 591, 3819–3830

616 76 Otto, G.P. *et al.* (2010) A Novel Syntaxin 6-Interacting protein, SHIP164, regulates
617 Syntaxin 6-Dependent sorting from early endosomes. *Traffic* 11, 688–705

618 77 Sueki, A. *et al.* (2020) Systematic Localization of Escherichia coli Membrane
619 Proteins. *mSystems* 5, e00808-19

620 78 Pettersen, E.F. *et al.* (2021) UCSF ChimeraX: Structure visualization for
621 researchers, educators, and developers. *Protein Sci.* 30, 70–82

622

Highlights

- VPS13, ATG2, SHIP164, Csf1 and the Hob proteins comprise a novel superfamily of conserved lipid transfer proteins with long hydrophobic grooves.
- All these long hydrophobic grooves are built from multiply repeating modules that consist of five β -sheets followed by a loop, for which we propose the name “repeating β -groove” (RBG) domain.
- RBG proteins carry out lipid transport at membrane contact sites, with functions in lipid homeostasis and membrane biogenesis. Some of these processes require bulk lipid transfer, which appears to be one of the primary molecular functions of RBG proteins.
- Eukaryotic RBG proteins likely evolved from structurally related prokaryotic proteins that transfer lipids between the inner and outer membranes in Gram-negative bacteria.

Outstanding Questions

- Which lipid classes can enter hydrophobic grooves? Only glycerophospholipids have been identified so far, but not sphingolipids or sterols. Does this apply generally?
- How are lipids selected? Box-like shuttling LTPs usually select for lipid headgroups, but RBG proteins show little headgroup selectivity *in vitro*. Instead, do they select lipid cargo by fatty acid composition, chain length, and/or saturation, since they interact mainly with acyl chains?
- What are the mechanisms that regulate the dynamics of lipid transfer by RBG proteins? RBG protein function requires multiple concurrent actions: targeting to appropriate membrane contact sites, ensuring no helices (which are likely highly mobile *in vivo*) block the tube, and crucially, generating a gradient that induces flow in one direction. How is all this regulated?
- How do structural properties of RBG proteins, like “springiness,” affect function? The ability to flex side-to-side or to stretch and compact vertically could play a role in RBG protein function.
- Is the lipid transfer function of RBG proteins conserved in bacteria? TamB, the best characterized RBG protein in bacteria, directly binds BamA, the insertase for outer membrane porins. This links TamB, and by implication the other bacterial RBG proteins, to export of porin β -strand polypeptides from inner to outer membranes. Could a similar polypeptide transfer function be present in eukaryote RBG proteins?

- What are the developmental and physiological functions of RBG proteins, and how does disruption of these functions cause disease? Cell biology experiments strongly suggest that mutation of RBG proteins leads to lipid imbalances. Yet, phenotypes in both unicellular and multicellular organisms are complex and not overtly related to lipids in many cases, implying quite indirect pathways to disease.

Figure 1

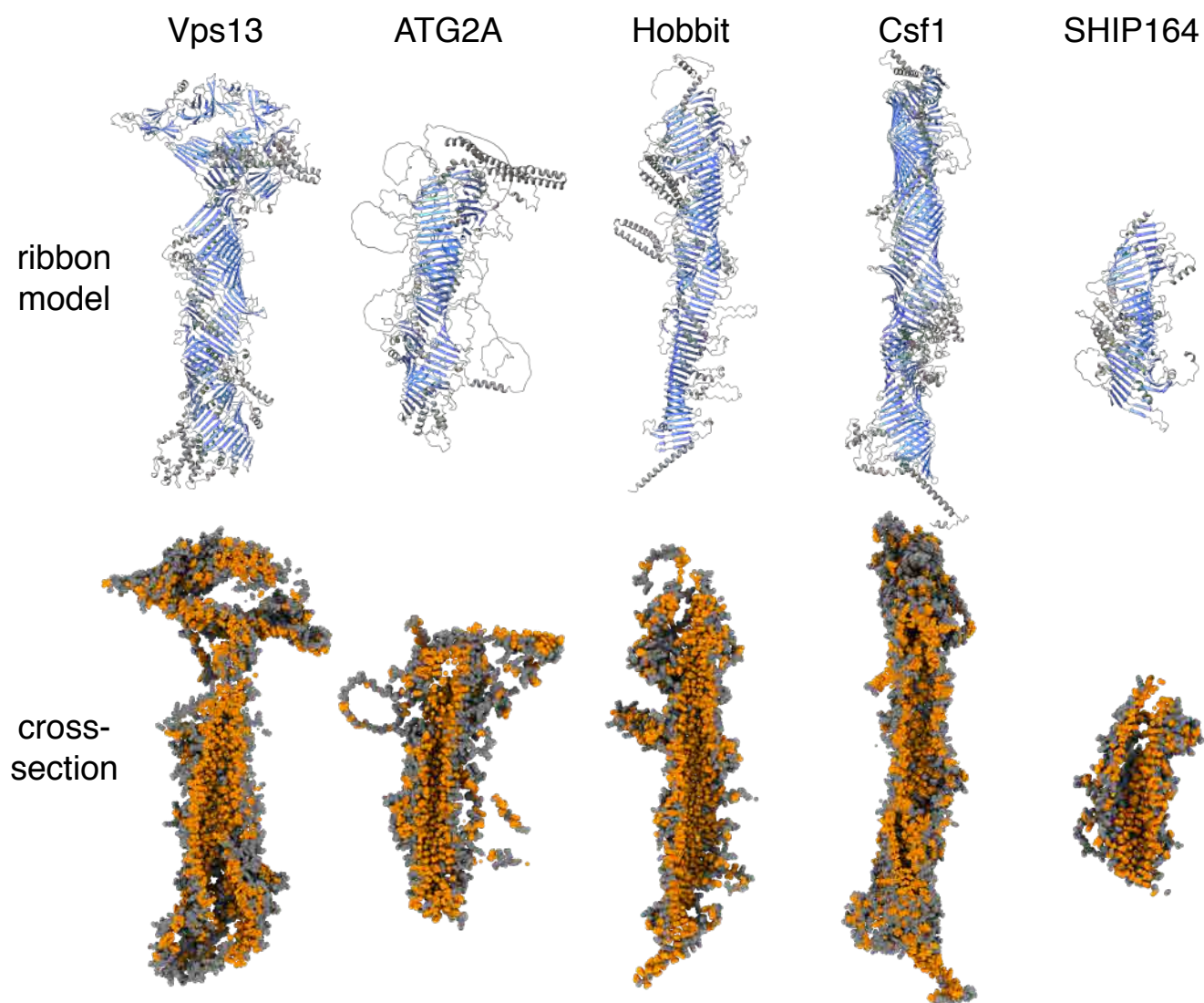


Figure 2

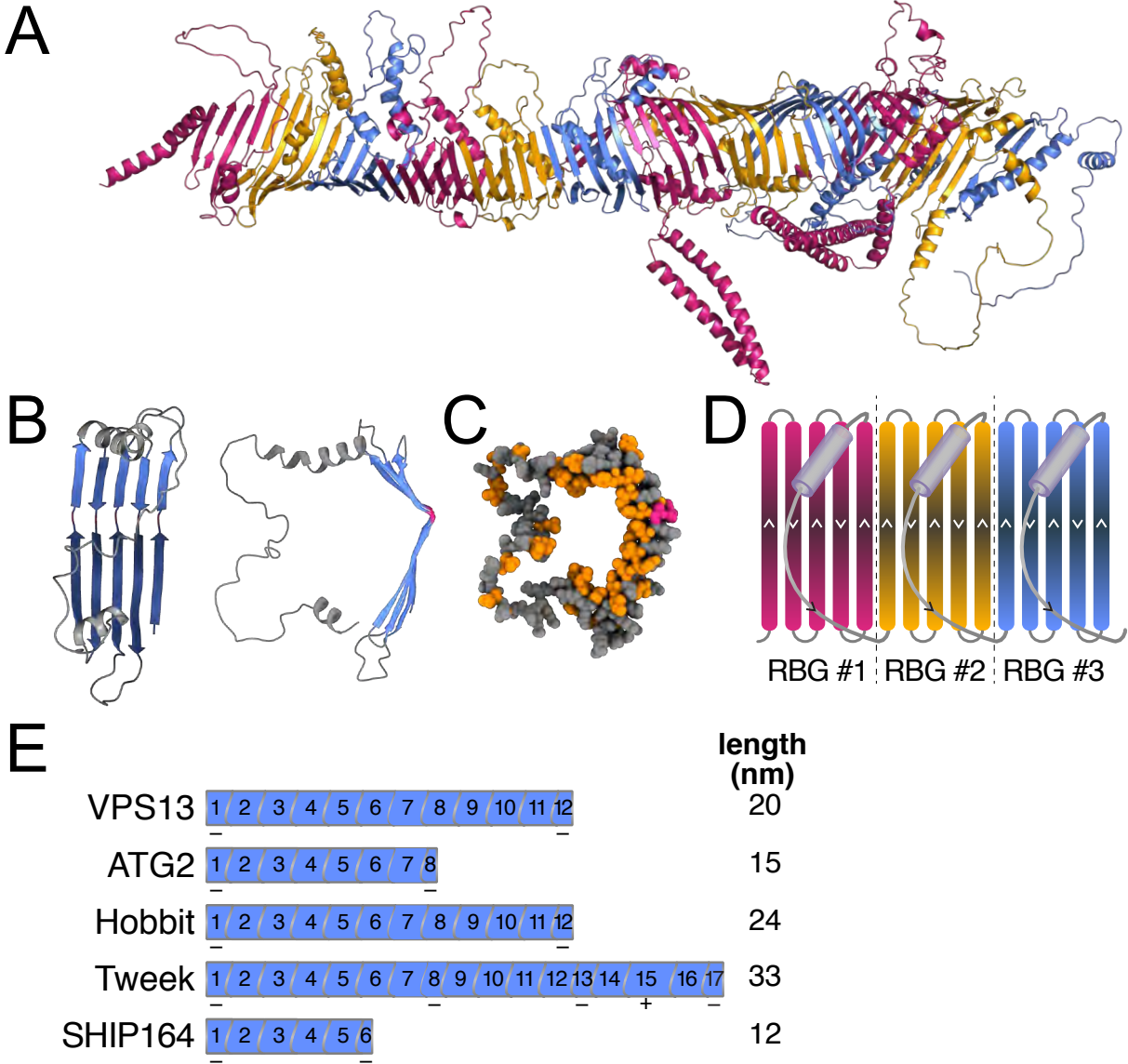
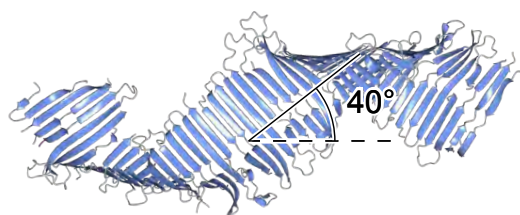


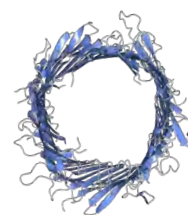
Figure 3

A

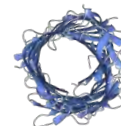
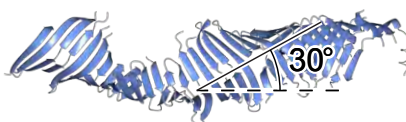
VPS13



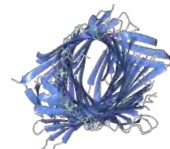
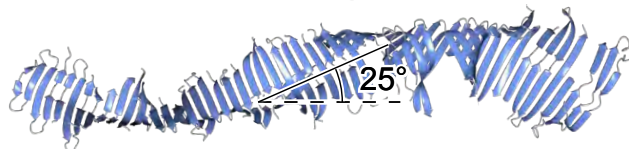
90°



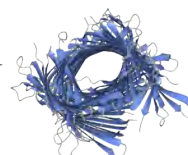
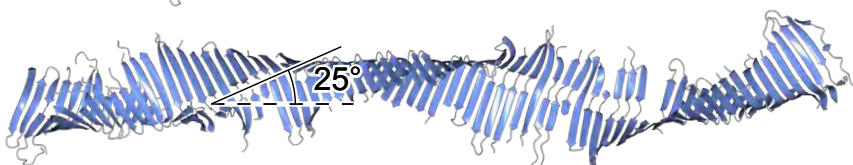
ATG2



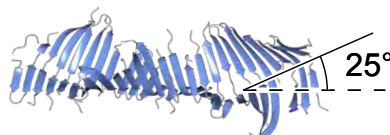
Hobbit



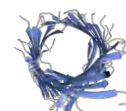
Tweek



SHIP164



10 nm



B

